J Mol Med (2002) 80:431–442
DOI 10.1007/s00109-002-0331-9

ORIGINAL ARTICLE

P. Lichtner · T. Attié-Bitach · S. Schuffenhauer
J. Henwood · P. Bouvagnet · P.J. Scambler
T. Meitinger · M. Vekemans

Expression and mutation analysis of *BRUNOL3*, a candidate gene for heart and thymus developmental defects associated with partial monosomy 10p

Received: 1 October 2001 / Accepted: 11 January 2002 / Published online: 4 April 2002

Abstract Partial monosomy 10p is a rare chromosomal aberration. Patients often show symptoms of the DiGeorge/velocardiofacial syndrome spectrum. The phenotype is the result of haploinsufficiency of at least two regions on 10p, the HDR1 region associated with hypoparathyroidism, sensorineural deafness, and renal defects (HDR syndrome) and the more proximal region DGCR2 responsible for heart defects and thymus hypoplasia/aplasia. While *GATA3* was identified as the disease causing gene for HDR syndrome, no genes have been identified thus far for the symptoms associated with DGCR2 haploinsufficiency. We constructed a deletion map of partial monosomy 10p patients and narrowed the critical region DGCR2 to about 300 kb. The genomic draft sequence of this region contains only one known gene, *BRUNOL3* (*NAPOR*, *CUGBP2*, *ETR3*). In situ hybridization of human embryos and fetuses revealed as well as in other tissues a strong expression of *BRUNOL3* in thymus during different developmental stages. *BRUNOL3* appears to be an important factor for thymus development and is therefore a candidate gene for the thymus hypoplasia/aplasia seen in partial monosomy 10p patients. We did not find *BRUNOL3* mutations in 92 DiGeorge syndrome-like patients without chromosomal deletions and in 8 parents with congenital heart defect children.

Keywords Partial monosomy 10p · DiGeorge syndrome · HDR syndrome · *BRUNOL3* · In situ hybridization

Abbreviations *BAC:* Bacterial artificial chromosome · *CHD:* Congenital heart defect · *DGS:* DiGeorge syndrome · *DHPLC:* Denaturing high-performance liquid chromatography · *FISH:* Fluorescent in situ hybridization · *HDR:* Hypoparathyroidism, deafness, renal anomalies · *PAC:* P1-derived artificial chromosome · *UTR:* Untranslated region · *VCFS:* Velocardiofacial syndrome · *wd:* Week of development

PETER LICHTNER recently completed his Ph.D. degree in chemistry at the University of Munich, Germany, for work on the DiGeorge syndrome locus on chromosome 10p. He is presently a postdoctoral fellow at the Institute of Human Genetics at the GSF National Research Center, Neuherberg, Germany. His research interests include mapping of susceptibility genes in complex diseases.

MICHEL VEKEMANS received his M.D. degree at the Université Catholique de Louvain, Belgium, and his Ph.D. degree in Genetics and Teratology from McGill University, Montreal, Canada. He is presently Professor of Genetics and Embryology at the Faculty de Médecine Necker, Université René Descartes, Paris, France. His research interests focus on the genetics of congenital malformations.

P. Lichtner (✉) · S. Schuffenhauer · T. Meitinger
Institute of Human Genetics, GSF National Research Center,
Ingolstädter Landstrasse 1, 85764 Neuherberg, Germany
e-mail: lichtner@gsf.de
Tel.: +49-89-31873525, Fax: +49-89-31873297

P. Lichtner · S. Schuffenhauer · T. Meitinger
Institute of Human Genetics, Klinikum Rechts der Isar,
Technical University, Munich, Germany

T. Attié-Bitach · M. Vekemans
Departement de Genetique et Unite INSERM U-393,
Hôpital Necker-Enfants Malades, Paris, France

J. Henwood
Molecular Medicine Unit, University of Leeds, Leeds, UK

P. Bouvagnet
Laboratoire de Genetique Moleculaire Humaine,
Faculte de Medecine Pharmacie,
Universite Claude Bernard Lyon 1, Lyon, France

P.J. Scambler
Molecular Medicine Unit, Institute of Child Health,
University College London, London, UK

Introduction

The DiGeorge syndrome (DGS)/velocardiofacial syndrome (VCFS) spectrum is a rather frequent human developmental disorder caused by abnormal development of the third and fourth pharyngeal pouches during embryogenesis [1] resulting in the three main symptoms congenital heart defect, hypoparathyroidism/hypocalcaemia, and thymus hypoplasia/aplasia or T cell defect, respectively.

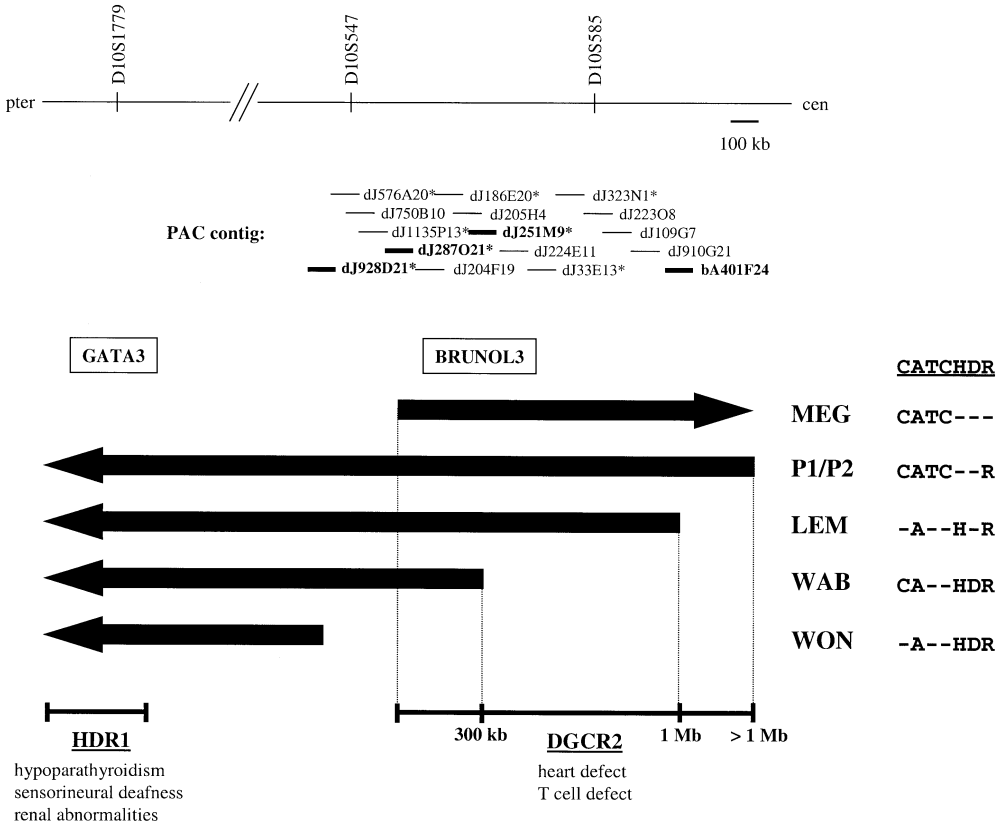

Fig. 1 Deletion map of patients with monosomy 10p. PAC clones (*bold*) indicate breakpoint spanning clones in the patients. PAC clones (*asterisks*) represent the minimal tiling path and were sequenced by the Sanger Centre. *Arrows* Regions deleted in patients; deletions continue in the direction of the arrowheads. Patients P1/P2 [4], LEM [5], WAB [13], and WON [7] had terminal deletions; patient MEG [12] had an interstitial deletion. The features of the patients are given according to the acronyms of the DGS/VCFS spectrum: *CATCH* cardiac defect, anomaly of face, thymic hypoplasia, cleft palate, hypocalcaemia/hypoparathyroidism; *HDR* hypoparathyroidism, deafness, renal anomaly. The regions for DGS (DGCR2) and HDR syndrome (HDR1) are indicated. The proximal boundary of the DGCR2 was defined in different publications by patients P1/P2 [4], LEM [7], and WAB (this report). The gene *GATA3* is responsible for the HDR syndrome, *BRUNOL3* is mapped within the least extended 300-kb region DGCR2 defined by patients MEG and WAB

The most important cause of DGS/VCFS is a 1.5 or 3 Mb microdeletion at chromosome 22q11 which occurs in 90% of cases. The estimated incidence is 1/4000 newborns [2, 3]. Reports of patients with partial monosomy 10p and features of this syndrome led to the definition of a second minor DGS/VCFS locus on the short arm of chromosome 10. Deletion studies in partial monosomy 10p patients mapped this locus in the vicinity of the markers D10S547 and D10S585 on 10p13/14 [4, 5, 6]. Later it became clear that the partial monosomy 10p phenotype could not be explained by haploinsufficiency of only a single region. A second more distal locus had to be postulated [7], meaning that the DGS-like phenotype associated with partial monosomy 10p is a contiguous gene syndrome. Haploinsufficiency of a distal region, termed HDR, is responsible for hypoparathyroidism, sensorineural deafness, and renal anomalies whereas haploinsufficiency of a more proximal region, designated DGCR2, contributes to the congenital heart defect and thymus hypoplasia/aplasia or T cell defect, respectively (Fig. 1).

Recently the molecular basis of the HDR1 phenotype was solved. It was shown that loss of function mutations of the *GATA3* gene result in the phenotype of hypoparathyroidism, sensorineural deafness, and renal anomalies, an autonomous clinical entity designated HDR syndrome [8]. The partial monosomy 10p subspectrum of heart defect and thymus hypoplasia/aplasia still remains unexplained. The DGCR2 locus associated with these two features maps about 4 Mb proximal to the *GATA3* gene. We established a P1-derived artificial chromosome (PAC) contig spanning the DGCR2 locus and constructed a deletion map of terminal and interstitial 10p deletions. In the course of the Human Genome Project the PAC contig was sequenced, and *in silico* analysis of the genomic sequence has focused the spotlight to a gene designated *NAPOR*, *ETR3*, *CUGBP2*, or *BRUNOL3* depending on how this gene had been isolated. *BRUNOL3* maps within the haploinsufficiency region DGCR2 and represents the first candidate gene for the heart defect and thymus hypoplasia/aplasia associated with partial monosomy 10p. In order to confirm the role of *BRUNOL3* for this developmental defect we performed both RNA in situ hybridization onto sections of human embryos and fetuses of various developmental stages and a mutation screen in chromosomal intact DGS/VCFS-like patients.

Table 1 Patients with symptoms of the DGS/VCFS spectrum. Malformations of the three organs heart, parathyroids, and thymus are listed separately. Developmental defects in these organs are associated with DGS/VCFS (*n* no abnormality detected, *PVS* pulmonary valve stenosis, *mVSD* membranous VSD, *DORV* double-outlet right ventricle, *RAA* right aortic arch, *TOF* tetralogy of Fallot, *IAA* interrupted aortic arch, *PA* pulmonary atresia, *PDA* persistent ductus arteriosus, *TA* truncus arteriosus, *TGV* transposition of great vessels, *C(L)P* cleft (lip) palate, *Vface* face typical of DGS/VCFS, *CA* coronary anomaly)

Patient no.	Heart	Parathyroids	Thymus	Other
1	TOF	n	n	CLP
2	IAA	Hypocalcaemia	n	Vface
3	VSD	n	n	Vface
4	Coarctation of aorta, aortic valve disruption	n	n	Vface
5	TOF	n	n	–
6	No data	No data	No data	“Typical VCFS”
7	Coarctation of aorta, hypoplastic aortic arch	n	n	–
8	TOF	n	n	–
9	IAA	Hypocalcaemia	Aplasia	–
10	IAA, mVSD	Hypoparathyroidism	Aplasia	Unilateral renal agenesis
11	IAA	Hypocalcaemia	Low T cells	Vface
12	mVSD	n	n	–
13	mVSD	n	n	Renal artery stenosis
14	TOF	Hypocalcaemia	n	Vface
15	DORV	n	n	–
16	IAA	n	n	Vface
17	n	n	n	Vface
18	VSD, ASD, PDA	Hypocalcaemia	n	–
19	VSD, PDA	n	n	–
20	VSD, PA	Hypoparathyroidism	Aplasia	CLP, cryptorchidism
21	PVS	Hypocalcaemia	Low T cells	cryptorchidism
22	TOF	n	n	Speech delay
23	PVS	n	n	Cleft soft palate
24	TOF			–
25	TOF, DORV	n	n	CLP, situs inversus
26	n	n	n	Vface, cleft soft palate
27	RAA, VSD	Hypocalcaemia	n	–
28	Double aorta	n	n	–
29	RAA, DORV, mVSD	Hypocalcaemia	Aplasia	Duane anomaly
30	TOF	n	n	–
31	PA, VSD	n	n	–
32	PA, VSD	n	n	Typical “conotruncal anomaly face”
33	PDA	Hypoparathyroidism	n	–
34	TOF	n	n	Vface
35	TOF	n	n	Vface
36	TOF	n	n	Hirschprung’s developmental delay
37	n	n	n	Vface, nasal speech
38	mVSD	n	n	Vface, nasal speech
39	n	n	n	Vface, nasal speech, speech delay
40	n	n	n	Vface, nasal speech
41	PA, VSD	n	Low T cells	Vface
42	Double aorta	n	n	CLP, ureteric reflux
43	IAA	n	n	Severe retardation
44	TOF, Ebstein’s anomaly	n	n	Choanal atresia
45	RAA	n	n	retardation, CP
46	n	Hypoparathyroidism	n	Deafness
47	mVSD	n	n	Nasal speech
48	IAA	Hypoparathyroidism	n	–
49	IAA	n	n	–
50	IAA	n	n	–
51	IAA	n	n	–
52	TA, IAA	n	n	–
53	TA	n	n	–
54	IAA	n	Low T cells	–
55	n	n	Aplasia	–
56	n	n	Aplasia	–
57	DORV	n	n	–
58	TGV	n	n	–

Table 2 Familial non-syndromic patients with conotruncal heart defects (for abbreviations see Table 1)

Patient no.	Heart	Other
59	TOF	–
60	PA, multiple VSD	–
61	mVSD	–
62	TOF	–
63	TOF	–
64	TOF	–
65	TOF	–
66	TOF	–
67	TOF	–
68	TGV; VSD	Cystic fibrosis
69	PVS, superior VSD, dextroposed aorta, bicuspid pulmonary valve	–
70	PA, VSD, major aortico-pulmonary collaterals	–
71	DORV, single coronary artery	–
72	PDA	–
73	PDA	–
74	PA, VSD	–
75	Mild PVS	–
76	Malposition of great vessels, tricuspid atresia	–
77	TOF	–
78	TOF	Facial dysmorphisms, mental retardation
79	TGV, VSD	–

Materials and methods

Fluorescent in situ hybridization studies

Metaphase spreads were prepared from cell lines according to standard procedures. Fluorescent in situ hybridization (FISH) was performed with PACs or bacterial artificial chromosomes (BACs) labelled by nick translation with biotin-14-dUTP (Sigma) and preannealed with Cot-1 DNA (Gibco BRL). Detection and visualization was achieved using the avidin-fluorescein isothiocyanate/anti-avidin antibody system described elsewhere [9, 10]. Chromosomes 10 were identified by 4-6-diamidino-2-phenylindole counterstaining. Breakpoint spanning clones were identified independently by two scientists on the basis of a reduced signal intensity on the deleted chromosome in comparison with the normal chromosome.

Northern blot

A hybridization probe from the 3′-untranslated region (UTR) of the *BRUNOL3* gene was generated by PCR (sense primer: 5′-CAA CCC ACC TGC ATG CAT CTC CC-3′, antisense primer: 5′-CAG AGT AGC ACA AGC CAA CTA TAA CCC-3′). The amplicon was 410 bp in length and was labelled by random-primed synthesis in the presence of [^{32}P]dCTP (Amersham Pharmacia Biotech) and used to probe a Human Cardiovascular System northern blot (Clontech, catalog no. 7791-1) with hybridization and washing conditions according to the manufacturer's protocol. Signals were detected by autoradiography.

In situ hybridization

Human conceptuses were collected from legally terminated pregnancies in agreement with the French law and ethics committee recommendations. Tissues were fixed with 4% paraformaldehyde, embedded in paraffin blocks, and sectioned at 5 µm. Due to the lack of sequence information for heart or thymus specific *BRUNOL3* isoforms we cloned a 410-bp PCR product of the 3′-UTR of *BRUNOL3* (corresponding to bp 4383–4792 of *NAPOR1* isoform, GenBank accession no. AF036956) into a pGEM-T vector (Promega). This probe detects the three *BRUNOL3* isoforms yet known. Sense and antisense riboprobes were generated using either SP6 or T7 RNA polymerase in the presence of [^{35}S]UTP (1200 Ci/mmol; NEN). Labelled probes were purified on Sephadex G50 columns. Hybridization and posthybridization washes were carried out according to standard protocols [11]. Slides were dehydrated, exposed to Biomax MR X-ray films (Amersham Pharmacia Biotech) for 3 days, dipped in Kodak NTB2 emulsion for 17 days at 14°C, developed, counterstained with toluidine blue, and coverslipped with Eukitt. Except for the pigmented retina no hybridization signal was detected with the sense probe, confirming that the in situ hybridization pattern of the antisense probe was specific.

Table 3 Patients with absent pulmonary valves. Patients were selected on the anatomical criteria of absent pulmonary valve. Other cardiovascular malformations are noted [*S* syndromic (i.e. with symptoms of DGS/VCFS), *NS* non-syndromic (i.e. without symptoms of DGS/VCFS, details are not known); for other abbreviations see Table 1]

Patient no.	Heart	Other
80	TOF	NS
81	TOF, RAA	NS
82	TOF, RAA	S
83	–	S
84	TOF	NS
85	TOF, RAA, CA	NS
86	TOF, infundibular VSD, CA	S
87	TOF, RAA, CA, aortic stenosis	S
88	TOF, RAA	NS
89	TOF	NS
90	TOF, inominate artery	NS
91	TOF, CA, right descending aorta, interrupted inferior vena cava	S
92	TOF	NS

Mutation screening

A total of 58 patients with symptoms of the DGS/VCFS (Table 1), 21 familial non-syndromic patients with conotruncal heart defects

(Table 2), and 13 patients with absent pulmonary valves together with other cardiovascular malformations (Table 3) were screened for mutations in the *BRUNOL3* gene. In addition, four married couples with two children showing congenital heart defects (CHD) were included in this study (Table 4). To exclude partial monosomy 22q11 FISH was performed using the cosmid N25 (D22S75) from the DGS deletion region on 22q11 (Appligene).

Exons were amplified from 100 ng genomic DNA by PCR using intronic primers (Table 5). Conditions for PCR amplification were 35 cycles of 94°C for 30 s, 60°C for 30 s, and 72°C for 30 s using a hot start polymerase (Amplitaq Gold, Perkin Elmer). The amplified products were analysed on a denaturing high-performance liquid chromatography (DHPLC) system (WAVE, Transgenomic) according to the manufacturer's protocol (Table 5). Samples with heteroduplex peaks in the chromatogram were sequenced using an ABI 377 sequencer.

Table 4 Parents of children with congenital heart defects; DNA of the children was not available for *BRUNOL3* mutation screening (for abbreviations see Table 1)

Parent nos.	Children with congenital heart defects
93, 94	One child with VSD, one child with TOF
95, 96	Two children with coarctation of aorta
97, 98	Two children with TOF
99, 100	One child with TOF, one child with coarctation of aorta

Results

Narrowing the haploinsufficiency region DGCR2

We established a PAC contig comprising of more than 100 clones spanning the haploinsufficiency region DGCR2. Eight clones representing a minimal tiling path were sequenced as part of the Human Genome Project by the Sanger Centre (dJ928D21, dJ576A20, dJ1135P13, dJ287O21, dJ186E20, dJ251M9, dJ33E13, dJ323N1; Fig. 1). By means of this contig we were able to identify breakpoint spanning PAC clones in three 10p deletion patients (MEG, WON, WAB). The breakpoint of one further patient (LEM) was characterized using mapping data from the Sanger Centre. Breakpoint spanning clones were identified in FISH experiments by comparing signal intensities of normal and deleted chromosomes. The distal boundary of the critical region DGCR2 was defined by patient MEG showing a heart defect and thymus hypoplasia [4, 5, 12]. PAC clone dJ287O21 was a breakpoint spanning clone in patient MEG. Patient LEM originally defined the proximal boundary of the DGCR2 [5]. BAC bA401F24 is spanning his breakpoint. This resulted in a critical region of approximately 1 Mb in size.

Table 5 Experimental conditions of *BRUNOL3* mutation screening. PCR products were analysed by DHPLC (WAVE, Transgenomic). The DHPLC conditions are as follows: gradient of Buffer B in within brackets followed by the oven temperature (buffer compositions according to the manufacturer's protocol)

Exon	Forward primer	Reverse primer	DHPLC
1A	CAG CAG ACA TCT AGC TCT GCC	GGC AAA GTG CCT AAT GAG TCG	(52–62)63 (51–61)65
1C	AGA GGG CGC GTT AGT GAG C	CAG CTC TAG AAA CTA GAA AAG CG	(51–61)57 (48–58)60 (43–53)62
2	CTT CCT GTC CCT CAT CGT GCC	CCA CCT GGA CGC CTG GCG	(54–64)62 (49–59)64 (39–49)67
3	AGC ATT CAC AGA AAT TTC TAA AAC C	TGA TTC TGG TAC AAA AGT AAA CCG	(48–58)57 (44–54)59
4	TCA ATC TGC CTT TAC TTT CTC CC	AGC AAG ACA GTT GGT TAC CAC C	(44–54)57 (44–54)58
5	GAA ATG GCC TTT GCT CAT TCG	AGC TCC AAT TAG CAC TGA AGG G	(51–61)58 (48–58)60 (45–55)62
6	GTT TAA CAA GCG TCC AAC CC	GAA AGG GCA GAT GAT ACA GTA C	(49–59)59 (46–56)61
7	TCC ACT TTC CAA TGT GTC TGA CC	AGT CAG TTT GCA GAG TTT CAG CG	(52–62)62 (50–60)64 (47–57)66
8	TCT CAC CAT CTC CAC TTT GCC	AGC ACG GTC AAA AGG AGA GGC	(47–57)61 (47–57)63 (43–53)65
9	TGC TGA AAG TAA CTT TCT CTT CCC	ACC TGC AAG GGA AGA GCA CCC	(51–61)61 (49–59)65
10	ACT CAC CTC GTG TCT TCT CTC CC	GAA GGC TGT CCA CCA GAG CAG C	(50–60)61 (48–58)62
11	TGC TGT TTC TCT TCT CTA TTG TTG GG	AGT GCT GCC TGT TGG GCT GGG	(52–62)66
12	ACT TTG GAA ACT AAG ACT CAA GGG	TGG GAA CCT ACT GCA ATA TAC TAG C	(53–63)57 (49–59)59
13	AGG CTG ACT CCC TCT CTC GG	ACT GGG TAG GGG AAG TGG G	(54–64)60 (52–62)61 (49–59)62

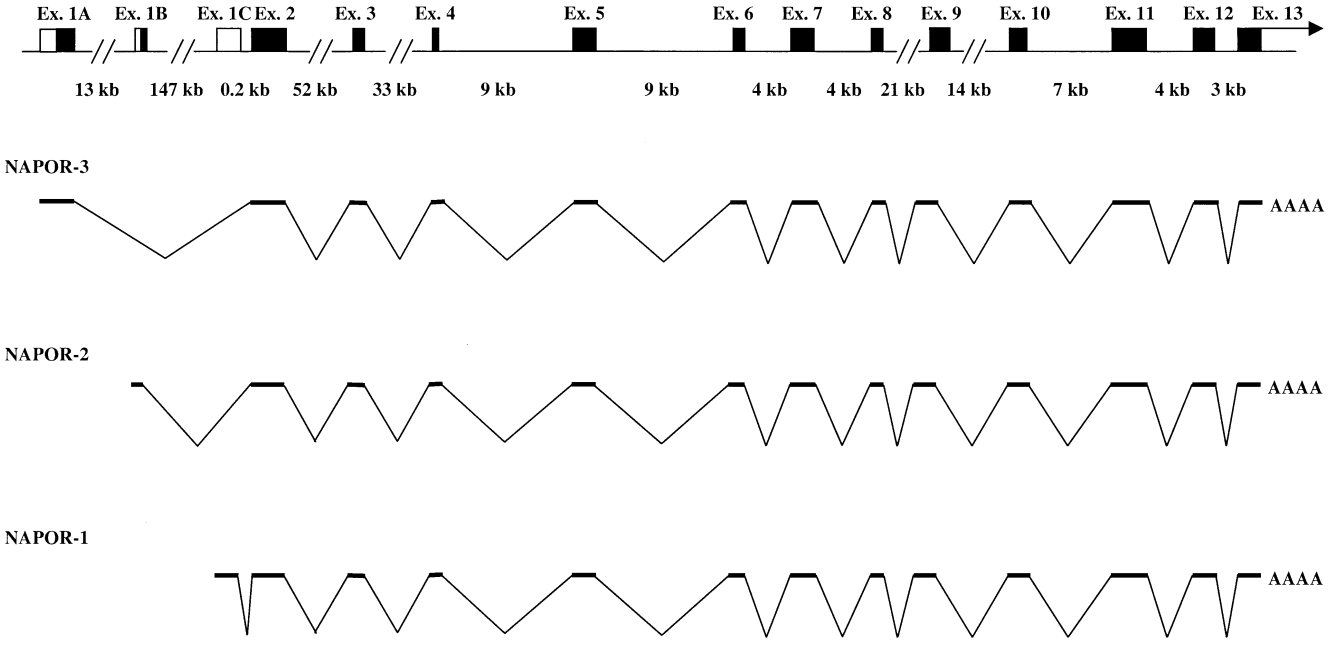

Fig. 2 Gene structure of the BRUNOL3 gene. Genomic organization of the three *BRUNOL3* isoforms *NAPOR1–3*. *Black boxes* Coding sequences; *white boxes* 5′-UTR. The gene structure refers to the *Homo sapiens* chromosome 10 working draft sequence segment NT_008705.3. Intron sizes are given in kilobases

We were able to further narrow this region by mapping the breakpoint of patient WAB. This patient has the HDR syndrome and in addition the DGCR2 associated malformation of the heart [13]. DJ251M9 was identified as a breakpoint spanning PAC clone in patient WAB shortening the critical region to about 300 kb.

PAC clone dJ928D21 is a breakpoint spanning clone in patient WON representing with an HDR syndrome without heart defect and without thymus hypoplasia/aplasia [7]. The breakpoint in this patient maps about 300 kb distal to the DGCR2 leaving him intact for the DGCR2 but deleted for the HDR1 region (Fig. 1).

BRUNOL3 expression during human development

In order to identify candidate genes for the heart disease and thymus hypoplasia/aplasia associated with haploinsufficiency of DGCR2 the genomic sequence of this region was analysed. The DGCR2 is located on the *Homo sapiens* chromosome 10 working draft sequence segment NT_008705.3. Thus far, only one known gene is mapped into this 300 kb DGCR2 interval, *BRUNOL3* (*NAPOR*, *CUGBP2*, *ETR3*). Genomic structure of *BRUNOL3* was determined *in silico* by comparing cDNA sequence with genomic sequence. The gene has 13 exons spanning a genomic region of more than 300 kb (Fig. 2). Three isoforms [GenBank accession nos. AF036956 (*NAPOR1*), AF090694 (*NAPOR2*), AF090693 (*NAPOR3*)] are known [14, 15], which differ predominantly in their first exons (exons 1A, 1B, 1C). Two further differences are a short 18 bp deletion in exon 11 of *NAPOR3* leading to a loss of six amino acids in the protein and a 1359-bp insertion in the 3′-UTR of *NAPOR3*. Nucleotides 1–15 of exon 1B of *NAPOR2* could not be found in the genomic sequence. Apart from that no sequence differences between cDNA sequence and genomic sequence were observed. All exon-intron boundaries are in accordance with the AT-GT consensus sequence.

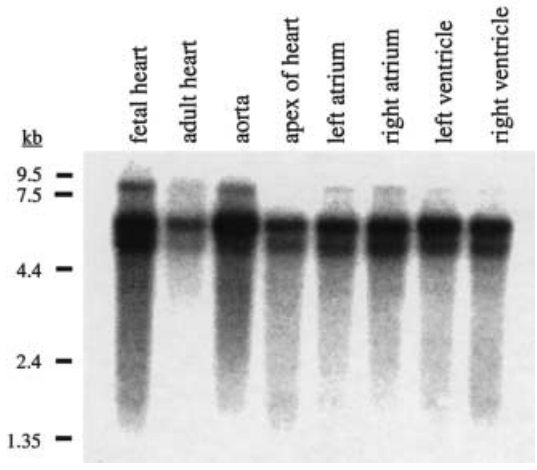

Fig. 3 Expression analysis in heart tissues. A northern blot with different heart tissues (Clontech) was hybridized with a radioactively labelled *BRUNOL3* probe. *Above the lanes* Tissues*; left* migration of RNA molecular size markers in kilobases. Signals are at 9, 6, 5, 4, and 1.5 kb

A hybridization probe was generated from a region of the *BRUNOL3* 3′-UTR that is identical in all three known isoforms of the gene (*NAPOR1–3*). We hybridized this probe onto a cardiovascular northern blot and detected at least five transcripts of different lengths, two strong signals at 6 kb and 5 kb and three weaker signals at 9, 4 and 1.5 kb. The signal patterns were identical in all heart tissues present on the northern blot (Fig. 3).

Table 6 Time course of tissue expression of *BRUNOL3* during human development (+ presence of *BRUNOL3* transcripts seen by in situ hybridization, – absence of transcripts, *?* data not available due to the level of the section, *x* structure does not exist at this stage, *wd* weeks of development, *d* days of development)

Tissue developmental stage	C12, 26d	C14, 32d	C16, 37d	C18, 44d	8 or 9 wd	15 wd	18 wd
Muscular system							
Myotome	++	++	++	x	x	x	x
Muscular cells in proximal limb buds	x	x	++	++	?	?	?
Kidney							
Mesonephros	++	++	+	?	x	x	x
Nephrons	x	x	?	?	++	++	++
Peripheral nervous system							
Dorsal root ganglia	+	++	++	++	?	?	?
Cranial nerve ganglia	x	?	++	++	?	?	?
Central nervous system							
Spinal cord	–	+	++	++	+++	+++	+++
Encephalon	–	+	++	++	?	+++	+++
Eye: optic vesicle then neural retina	?	?	?	?	+++	+++	+++
Ear: otic vesicle then internal ear	–	?	++	++	?	?	?
Heart	–	–	–	–	+	?	+?
Digestive and respiratory system	–	?	+	++	++	?	?
Thymus	x	x	x	+?	+++	?	+++

To obtain a more precise expression profile of *BRUNOL3* during human development we performed RNA in situ hybridization onto sections of human embryos ranging from Carnegie C10–C18. No *BRUNOL3* expression was detected at Carnegie stage C10, the youngest developmental stage studied (not shown). From Carnegie stage C12 to C18 a *BRUNOL3* expression was observed in various tissues and organs (Table 6). The highest expression was observed in myotome (Fig. 4AA,CC) then migrating muscular cells of proximal limb buds (Fig. 4DD). Transcripts were also detected in peripheral nervous system (dorsal root ganglia and cranial nerve ganglia, Fig. 4A–C) and in the central nervous system (medial part of neural tube and encephalon, Fig. 4CC, EE) and this signal increased during development. A signal was also observed in the mesonephros by C12 (Fig. 4AA′) that decreased later, in the otic vesicle at C14 and C16 (Fig. 4EE′), in the apical ectodermal ridge of limb buds at C14 and C16 (Fig. 4BB′, DD′), in the muscular layer of oesophagus (Fig. 4BB′), stomach and intestine (not shown) and around the trachea by C16 (Fig. 4BB′). No *BRUNOL3* expression was detected in the developing heart during these embryonic stages. We then studied four more fetal stages [8th, 9th, 15th and 18th week of development (wd)] concentrating our attention to the heart and thymus because defects in these organs are associated with haploinsufficiency of DGCR2, and to the central nervous system because of the strong signal observed during embryogenesis. The strongest *BRUNOL3* expression was found in thymus from the 8th to 18th wd (Fig. 4F–G′, JJ′). In the central nervous system, a strong *BRUNOL3* expression was seen in the neural retina (Fig. 4HH′, RR′), the dorsal horns of the spinal cord (Fig. 4OO′), the cerebral cortex, the ventricular zone and the germinal matrix (Fig. 4QQ′), the hippocampus (Fig. 4PP′) and the basal ganglia (not shown). In the heart an expression was observed in the 9th wd both in ventricles and auricles but not in great vessels except at the tip of the pulmonary artery (Fig. 4II′). A weak heart expression was also suspected on the autoradiography in the 8th wd (Fig. 4FF′) and 18th wd (not shown) but could not be confirmed after analysis of the slides (no signal above the background). Finally, we also detected *BRUNOL3* transcripts in the muscular layer of digestive tract (Fig. 4K–L′), epithelium of bronchial bud (Fig. 4MM′) and nephrons of the kidney (Fig. 4NN) during fetal development (results are summarized in Table 6).

Table 7 List of polymorphisms in the *BRUNOL3* gene. Sequence variations were found in 7 of 14 exons screened for mutations in 96 patients. Nomenclature corresponds to the recommendations of the Nomenclature Working Group [16, 17]. Reference cDNA is *NAPOR1* (GenBank accession no. AF036956)

Exon	Sequence variations	Variations/wt	%
1A	No variants	0/100	–
1C	c.-133–132insC	16/84	16
	c.-172G>A	1/99	1
2	IVS2+6G>T	1/99	1
	IVS2+6G>A	1/99	1
3	no variants	0/100	–
4	No variants	0/100	–
5	c.345T>A	25/75	25
	c.348G>A	1/99	1
6	No variants	0/100	–
7	IVS7+28C>A	3/97	3
8	No variants	0/100	–
9	IVS9+10G>A	48/52	48
10	c.1165C>T	34/66	34
11	No variants	0/100	–
12	IVS11–18delT	47/53	47
13	No variants	0/100	–

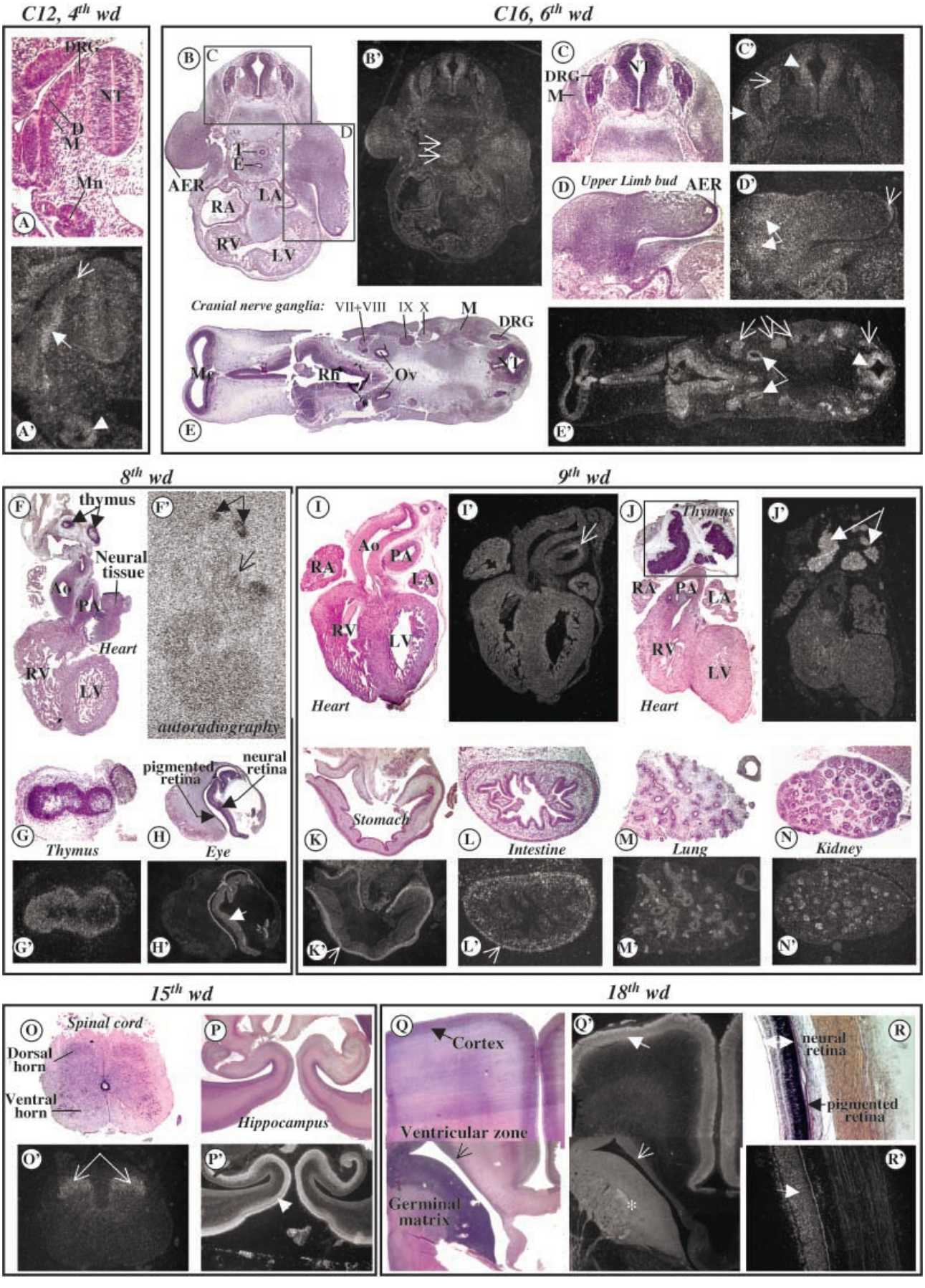
C12, 4th wd
C16, 6th wd
8th wd
9th wd
15th wd
18th wd
DRG
NT
D
M
Mn
A
A'
B
C
B'
C'
AER
RA
LA
RV
LV
T
E
D'
Upper Limb bud
Cranial nerve ganglia:
VII+VIII
IX X
Mc
Rh
Ov
E
E'
thymus
Neural tissue
Ao
PA
Heart
F
F'
autoradiography
pigmented retina
neural retina
Thymus
Eye
G
H
G'
H'
I
I'
J
J'
Stomach
Intestine
Lung
Kidney
K
L
M
N
K'
L'
M'
N'
Spinal cord
Dorsal horn
Ventral horn
O
O'
P
P'
Hippocampus
Q
Cortex
Ventricular zone
Germinal matrix
Q'
R
R'

BRUNOL3 mutation screening in chromosomal normal DGS-like patients

We screened a group of 92 DGS-like patients and 8 parents with children presenting with congenital heart defects for *BRUNOL3* mutations by PCR amplification and subsequent DHPLC analysis of all exons except exon 1B where a discrepancy between cDNA sequence and genomic sequence was observed. All patients had symptoms of the DGS. Microdeletions on 22q11 and partial monosomies 10p had been excluded. The majority of patients showed congenital heart defects. A thymus abnormality was observed in ten patients. A thymus hypoplasia was demonstrated in six of these patients; four patients had low T cell numbers (Tables 1, 2, 3, 4). The mutation screening in this collection of DGS-like patients revealed ten sequence variations in seven exons of *BRUNOL3* (Table 7). None of these were obvious pathogenic mutations. Seven variations are located in intronic regions or in the 5′-UTR, three variations are one basepair substitutions in coding sequences leaving the amino acid sequences unchanged.

◀ **Fig. 4A–R** *BRUNOL3* expression during human development. **A**–**R** Bright-field illumination of haematoxylin/eosin stained slides, adjacent to the ones presented for the in situ hybridization studies under dark-field illumination (**A′**–**R′**), except **F′** which is the autoradiography of the hybridized slide. Age are given in weeks of development (*wd*). **AA′** C12, 4th wd embryo. Expression is seen in the myotome (*M*, *arrow*), the dorsal root ganglia (*DRG*, *thin arrow*) and the mesonephros (*Mn*, *arrowhead*). **B**–**E′** C16, 6th wd embryo. **CC′** and **DD′** are a high magnification view of **BB′**. **CC′**, **EE′** show *BRUNOL3* expression in the medial part of neural tube, on either parts of sulcus limitans (*arrowhead*), in dorsal root ganglia (*thin arrow*) and in the myotome (*thick arrow*). **DD′** show a gene expression in proximal limb buds (migrating myotomal cells) and distally in the apical ectodermal ridge (*AER*). *BRUNOL3* is also expressed around the trachea (*T*) and the oesophagus (*E*) as seen in **BB′** (*arrows*). **EE′** transverse section through the head, where an expression is observed in the rhombencephalon (*Rh*), mesencephalon (*Me*), the otic vesicles (*Ov*, *arrows*), the cranial nerve (VII+VIII, IX, X) and dorsal root ganglia (*thin arrow*). No *BRUNOL3* expression was detected in the developing heart. *RA* Right auricle; *LA* left auricle; *RV* right ventricle; *LV* left ventricle. **F**–**H′** 8th wd sections. **FF′** Frontal section through the heart and thymus, showing a *BRUNOL3* expression at the tip of the pulmonary artery (*PA*, *thin arrow*) and in thymus (*arrows*) on the autoradiography, confirmed after analysis of the slides (**GG′**). A weaker *BRUNOL3* expression was also suspected in the heart on the autoradiography but could not be confirmed under dark field illumination (no signal above the background). *Ao* Aorta. Expression is also shown in the neural retina (**HH′**, note the false-positive signal in pigmented retina). **I**–**N** 9th wd sections. **II′** frontal section of the heart showing *BRUNOL3* expression in both ventricles but not in great vessels, except at the tip of the pulmonary artery (*thin arrow*). **JJ′** frontal section of the heart and thymus showing a strong expression in the thymus as compared to the heart (weak expression) and the pulmonary artery (no expression). *BRUNOL3 transcripts* were also observed in the muscular layer of stomach and intestine (**KK′**, **LL′**), the epithelia respiratory trees (**MM′**) and in the nephrons of the kidney (**NN**). **O**–**P′** 15th wd sections. *BRUNOL3* expression in the dorsal horns of the spinal cord (**OO′**) and the hippocampus (**PP′**). **Q**–**R′**: 18th wd sections. *BRUNOL3* is expressed in the entire cerebral cortex including the frontoparietal cortex (*arrow*), the ventricular zone (*thin arrow*), the germinal matrix (*asterisk*, **QQ′**) and in the basal ganglia (thalamus, not shown). **RR′** parasagittal section of the eye where *BRUNOL3* is still expressed in the neural retina

Discussion

The haploinsufficiency region DGCR2

Partial monosomy 10p is a rare chromosomal aberration. Until now about 50 cases have been reported in the literature [18]. A significant number of these patients present with features of DGS, such as heart defects, thymus hypoplasia/aplasia and T cell defects or with hypoparathyroidism/hypocalcaemia and other features. These symptoms are typical of the DGS/VCFS. That is why a second minor DGS/VCFS locus (DGCR2) on 10p was postulated and mapped near marker D10S585 by 10p deletion analysis in terminally and interstitially deleted patients [4, 5, 6]. It was later shown that the phenotype of partial monosomy 10p was indeed due to haploinsufficiency of at least two regions, the HDR1 region responsible for HDR syndrome and the more proximal region DGCR2 responsible for the heart defect and thymus hypoplasia/aplasia [7]. The HDR syndrome causing gene *GATA3* was identified by mutation screenings in HDR patients without 10p deletions. Loss of function mutations in *GATA3* were found in three HDR syndrome patients [8]. Genes from the DGCR2 causing heart defects and thymus hypoplasia/aplasia or T cell defects were unknown yet. The region was originally defined by deletion mapping with FISH using YAC clones as probes.

Patients MEG and P1/P2 who presented with heart defects and T cell defects showed the smallest region of overlapping deletions leading to a size of more than 1 Mb for the DGCR2 [4]. A second study narrowed the critical region to about 1 Mb by the new patient LEM, who defined the proximal boundary of DGCR2 [5]. As in the first study the distal boundary was defined by patient MEG. It is known from several studies that there is a wide variability in the phenotypic features of patients with deletions or duplications of the same chromosomal region, such as partial monosomy 4p in patients with Wolf-Hirschhorn syndrome, partial monosomy 5p in cri du chat syndrome, and partial monosomy 22q11 in DGS. For this reason the presence of a particular trait carries more weight than its absence. Patient LEM presented with hypoparathyroidism and renal defects but had neither a heart defect nor a T cell defect. Thus patient LEM showed symptoms of the HDR syndrome but no symptoms associated with the DGCR2 and was therefore ill suited in defining the DGCR2. Recently we studied the breakpoint of patient WAB, who was published as a patient with HDR syndrome [7]. Her symptoms of hypoparathyroidism, sensorineural deafness, and renal defect belong to the HDR syndrome and are most likely the result of haploinsufficiency of *GATA3* mapped within the HDR1 haploinsufficiency locus. In addition, this patient showed a heart defect. The symptom of a heart defect is not associated with the HDR1 region but with haploinsufficiency of the more proximal region DGCR2. For this reason, WAB is qualified for defining the critical region DGCR2.

We mapped WAB's breakpoint about 300 kb proximal to the distal DGCR2 boundary defined by MEG. This narrows the size of the DGCR2 to about 300 kb. A T cell defect is not observed in WAB. This is not unusual, however, because a high variability in phenotypic expression and low penetrance is well known in partial monosomy 10p patients. Also it cannot be excluded that the symptoms heart defect and thymus hypoplasia/aplasia are the result of haploinsufficiency of more than one gene within the DGCR2. A gene responsible for heart defects may be located in the distal part of the DGCR2 and a gene responsible for the thymus hypoplasia/aplasia may be located in a more proximal region that is not deleted in WAB. The breakpoint of the recently published HDR syndrome patient WON could be mapped to a PAC clone that is located about 300 kb distal to the DGCR2. She is hemizygous for the HDR1 region and *GATA3* but dizygous for the DGCR2 haploinsufficiency region. Her 10p deletion accounts for the HDR syndrome phenotype and the absence of a heart defect and a thymus hypoplasia/aplasia or T cell defect, respectively.

Within the 300-kb region defining the DGCR2 only one known gene, *BRUNOL3*, was identified in the human genome draft sequence. It is a homolog of the *Drosophila bruno* gene and belongs to a protein superfamily of RNA binding proteins [19]. Drosophila bruno is a key factor for *Drosophila* embryo development [20, 21]. Furthermore there are several examples where defective RNA binding proteins lead to different developmental defects in various species [22, 23, 24, 25]. This and the fact that it mapped within the DGCR2 made *BRUNOL3* a candidate gene for the heart defect and thymus hypoplasia/aplasia or T cell defect observed in partial monosomy 10p patients.

Expression profile of the *BRUNOL3* gene during human development

At present there are three isoforms of the gene in the database (*NAPOR1–3*) differing predominantly in their first exons [26]. We confirmed the presence of several isoforms by hybridizing a cardiovascular northern blot with a *BRUNOL3* probe. Moreover, an expressed sequence tag database search with the *BRUNOL3* cDNA reveals expression in more than 20 different tissues. In order to decide whether *BRUNOL3* mutations might be responsible for the heart defect and thymus hypoplasia/aplasia in partial monosomy 10p patients we established an expression profile of *BRUNOL3* during early human development. The strongest expression was observed in the muscular system, the central nervous system and the thymus, suggesting that *BRUNOL3* plays an important role in human thymus development. This makes *BRUNOL3* a candidate gene for the thymus hypoplasia/aplasia or T cell defect often seen in 10p deletion patients. On the other hand a weaker expression in the heart was observed in the 9th wd, but we could not confirm a heart expression at other developmental stages. This is contrary to another report in which a strong expression of *BRUNOL3* in the developing heart was described [27].

It is important to mention that our in situ hybridizations were performed on a selection of developmental stages only, and that we cannot exclude *BRUNOL3* expression in stages other than described here. However, the most likely explanation for these inconsistent results is that specific isoforms are expressed in the developing heart and that our hybridization probe from the 3′-UTR failed to detect these isoforms. It was shown that both in mice and chickens there is a transition from high to low molecular weight *BRUNOL3* isoforms during heart development [27]. This is why our hybridization results do not exclude a suggested role of *BRUNOL3* in heart development. Apart from thymus and heart, *BRUNOL3* expression was observed in several other tissues and organs, mainly the central nervous and muscular systems, but also in the digestive tract, lung and kidney. These organs are usually not affected in partial monosomy 10p patients. This might be due to a lower gene dose sensitivity in these organs or due to a compensation of *BRUNOL3* by homologous genes. A good candidate would be *BRUNOL2* that has an 80% amino acid identity with *BRUNOL3* over the entire length of the protein.

Mutation screening of the *BRUNOL3* gene in DGS/VCFS-like patients

Despite the fact that no strong *BRUNOL3* expression was observed in the heart a role of the gene in heart development cannot be excluded. Indeed, it has been demonstrated that *BRUNOL3* regulates alternative splicing of specific genes during heart development in chickens and mice [27]. In contrast, our in situ hybridization experiments revealed a strong *BRUNOL3* expression in the human thymus at different developmental stages. Taking expression and mapping data together, *BRUNOL3* represents a candidate gene for thymus and/or heart defects. Therefore we screened 92 patients with CHD and/or thymus hypoplasia and 8 parents with CHD children for *BRUNOL3* mutations. None of these patients had a microdeletion on 22q11 or deletion on 10p. As discussed previously, the symptoms heart defect and thymus hypoplasia/aplasia could be the result of haploinsufficiency of more than one gene within the DGCR2. *BRUNOL3* could be responsible for the thymus hypoplasia/aplasia, and the gene responsible for the heart defects may be located in the distal part of the DGCR2. However, the majority were selected for congenital heart defects. Patients with thymus hypoplasia/aplasia are very rare, and only six of these patients had clear thymus hypoplasia/aplasia, two of them as an isolated symptom. In addition, four more patients had low T cell numbers. Mutations in the *BRUNOL3* gene were not identified. In addition to technical limitations of the PCR-based screening method that made it impossible, for example, to identify intragenic deletions and the fact that we did not analyse regulatory regions, there are several possible reasons why no

Table 8 List of genes surrounding the haploinsufficiency region DGCR2: genes mapped within or close to the DGCR2, and that are included in the Human Genome Project Working Draft at UCSC of this region. The order of genes is from distal (*top*) to proximal (*bottom*). *BRUNOL3* is the only gene mapped within the least extended DGCR2 (300 kb) and was analysed in this report

Gene	Short description
BRUNOL3 (*NAPOR*, *ETR3*, *CUGBP2*)	RNA-binding protein related to the Drosophila Bruno translational regulator
KIAA0019 (*RNTRE*)	RAB5 GTPase-activating protein (GAP); involved in EGFR signalling pathway
RENT2	Regulator of nonsense-mediated decay of aberrant mRNAs containing premature termination codons
FLJ10578	Homolog of *S. cerevisiae* Sec61p, the main ribosome receptor in the ER; involved in co-translational membrane targeting
NUDT5	Nudix hydrolase; converts ADP-ribose to AMP or ribose 5-phosphate
LOC57118	CamKI-like protein kinase; granulocyte specific; activates ERK/MAP kinase activity

mutations were found. *BRUNOL3* is a gene with many isoforms usually due to alternative splicing [26]. During heart development there is a switch from high to low molecular weight isoforms [27]. It is possible that we missed one or more still unidentified exons in our mutation screening that are specifically expressed during heart and thymus development. In addition the DGS-like phenotype might be the result of environmental and genetic factors. It is known that teratogens and pregnancy factors such as alcohol and retinoids or diabetes in the mother may also lead to this developmental defect [1, 28, 29]. It must also taken into account that CHD is a very heterogeneous condition. Therefore the number of patients investigated might be too small to find mutations.

Future prospects

Haploinsufficiency of the DGCR2 is associated with heart defects and thymus hypoplasia/aplasia. Patient WAB narrowed this critical region to about 300 kb. So far only the gene *BRUNOL3* has been mapped within this interval. This and the fact that *BRUNOL3* is expressed in the developing heart and thymus made it a candidate gene for the observed phenotype of partial monosomy 10p patients. Patient WAB, who defined the proximal boundary of the DGCR2 showed a heart defect. However, it cannot be excluded that there are more regions on chromosome 10p responsible for congenital heart defects and that the heart defect in patient WAB is due to haploinsufficiency of a gene distal to the DGCR2. It is also possible that the heart defect in this patient is the result of a position effect and that the DGCR2 is larger than 300 kb. It was originally defined by patients MEG and P1/P2 and had a size of about 2 Mb [4] (Fig. 1). At least five more genes are mapped within this region (Table 8). These genes are candidate genes for the heart defect and thymus hypoplasia/aplasia as well. Expression profiles of all genes will give clues whether they may play a role during heart and thymus development. Good candidate genes could then be screened for mutations in chromosomal normal DGS-like patients. If no mutations are found, the possibility may remain to generate heterozygous +/– knockout mice for candidate genes and to compare the murine with the human phenotype. This was a successful approach for the DGS locus on chromosome 22q11, where *Tbx1* +/– mice developed the cardiovascular defects typical of the DGS/VCFS [30, 31, 32].

Acknowledgements We thank Joelle Augé for technical assistance and Férechté Encha-Razavi for helpful discussion. This study was supported in part by Deutsche Forschungsgemeinschaft (P.L., S.S., T.M.), EUREXpress (T.A.-B., M.V.), and the British Heart Foundation (P.J.S.).

References

1. Lammer EJ, Opitz JM (1986) The DiGeorge anomaly as a developmental field defect. Am J Med Genet Suppl 2:113–127
2. Carey AH, Kelly D, Halford S, Wadey R, Wilson D, Goodship J, Burn J, Paul T, Sharkey A, Dumanski J, et al (1992) Molecular genetic study of the frequency of monosomy 22q11 in DiGeorge syndrome. Am J Hum Genet 51:964–970
3. Driscoll DA, Salvin J, Sellinger B, Budarf ML, McDonald-McGinn DM, Zackai EH, Emanuel BS (1993) Prevalence of 22q11 microdeletions in DiGeorge and velocardiofacial syndromes: implications for genetic counselling and prenatal diagnosis. J Med Genet 30:813–817
4. Daw SC, Taylor C, Kraman M, Call K, Mao J, Schuffenhauer S, Meitinger T, Lipson T, Goodship J, Scambler P (1996) A common region of 10p deleted in DiGeorge and velocardiofacial syndromes. Nat Genet 13:458–460
5. Schuffenhauer S, Lichtner P, Peykar-Derakhshandeh P, Murken J, Haas OA, Back E, Wolff G, Zabel B, Barisic I, Rauch A, Borochowitz Z, Dallapiccola B, Ross M, Meitinger T (1998) Deletion mapping on chromosome 10p and definition of a critical region for the second DiGeorge syndrome locus (DGS2). Eur J Hum Genet 6:213–225
6. Gottlieb S, Driscoll DA, Punnett HH, Sellinger B, Emanuel BS, Budarf ML (1998) Characterization of 10p deletions suggests two nonoverlapping regions contribute to the DiGeorge syndrome phenotype. Am J Hum Genet 62:495–498
7. Lichtner P, Konig R, Hasegawa T, Van Esch H, Meitinger T, Schuffenhauer S (2000) An HDR (hypoparathyroidism, deafness, renal dysplasia) syndrome locus maps distal to the DiGeorge syndrome region on 10p13/14. J Med Genet 37:33–37
8. Van Esch H, Groenen P, Nesbit MA, Schuffenhauer S, Lichtner P, Vanderlinden G, Harding B, Beetz R, Bilous RW, Holdaway I, Shaw NJ, Fryns JP, Van de Ven W, Thakker RV, Devriendt K (2000) GATA3 haplo-insufficiency causes human HDR syndrome. Nature 406:419–422
9. Lichter P, Cremer T, Borden J, Manuelidis L, Ward DC (1988) Delineation of individual human chromosomes in metaphase and interphase cells by in situ suppression hybridization using recombinant DNA libraries. Hum Genet 80:224–234

10. Lichter P, Tang CJ, Call K, Hermanson G, Evans GA, Housman D, Ward DC (1990) High-resolution mapping of human chromosome 11 by in situ hybridization with cosmid clones. Science 247:64–69
11. Wilkinson DG (1992) In situ hybridization: a practical approach. Oxford University Press, Oxford
12. Lipson A, Fagan K, Colley A, Colley P, Sholler G, Issacs D, Oates RK (1996) Velo-cardio-facial and partial DiGeorge phenotype in a child with interstitial deletion at 10p13–implications for cytogenetics and molecular biology. Am J Med Genet 65:304–308
13. Hasegawa T, Hasegawa Y, Aso T, Koto S, Nagai T, Tsuchiya Y, Kim KC, Ohashi H, Wakui K, Fukushima Y (1997) HDR syndrome (hypoparathyroidism, sensorineural deafness, renal dysplasia) associated with del(10)(p13). Am J Med Genet 73:416–418
14. Choi DK, Ito T, Tsukahara F, Hirai M, Sakaki Y (1999) Developmentally-regulated expression of mNapor encoding an apoptosis-induced ELAV-type RNA binding protein. Gene 237:135–142
15. Lu X, Timchenko NA, Timchenko LT (1999) Cardiac elav-type RNA-binding protein (ETR-3) binds to RNA CUG repeats expanded in myotonic dystrophy. Hum Mol Genet 8:53–60
16. Antonarakis SE (1998) Recommendations for a nomenclature system for human gene mutations. Nomenclature Working Group. Hum Mutat 11:1–3
17. Dunnen JT, Antonarakis SE (2000) Mutation nomenclature extensions and suggestions to describe complex mutations: a discussion. Hum Mutat 15:7–12
18. Van Esch H, Groenen P, Fryns JP, Van de Ven W, Devriendt K (1999) The phenotypic spectrum of the 10p deletion syndrome versus the classical DiGeorge syndrome. Genet Couns 10:59–65
19. Good PJ, Chen Q, Warner SJ, Herring DC (2000) A family of human RNA-binding proteins related to the Drosophila Bruno translational regulator. J Biol Chem 275:28583–28592
20. Ephrussi A, Lehmann R (1992) Induction of germ cell formation by oskar. Nature 358:387–392
21. Kim-Ha J, Kerr K, Macdonald PM (1995) Translational regulation of oskar mRNA by bruno, an ovarian RNA-binding protein, is essential. Cell 81:403–412
22. Yao KM, Samson ML, Reeves R, White K (1993) Gene elav of Drosophila melanogaster: a prototype for neuronal-specific RNA binding protein gene family that is conserved in flies and humans. J Neurobiol 24:723–739
23. Lundquist EA, Herman RK, Rogalski TM, Mullen GP, Moerman DG, Shaw JE (1996) The mec-8 gene of C. elegans encodes a protein with two RNA recognition motifs and regulates alternative splicing of unc-52 transcripts. Development 122:1601–1610
24. Ebersole TA, Chen Q, Justice MJ, Artzt K (1996) The quaking gene product necessary in embryogenesis and myelination combines features of RNA binding and signal transduction proteins. Nat Genet 12:260–265
25. Macknight R, Bancroft I, Page T, Lister C, Schmidt R, Love K, Westphal L, Murphy G, Sherson S, Cobbett C, Dean C (1997) FCA, a gene controlling flowering time in Arabidopsis, encodes a protein containing RNA-binding domains. Cell 89:737–745
26. Choi DK, Ito T, Mitsui Y, Sakaki Y (1998) Fluorescent differential display analysis of gene expression in apoptotic neuroblastoma cells. Gene 223:21–31
27. Ladd AN, Charlet N, Cooper TA (2001) The CELF family of RNA binding proteins is implicated in cell-specific and developmentally regulated alternative splicing. Mol Cell Biol 21:1285–1296
28. Ammann AJ, Wara DW, Cowan MJ, Barrett DJ, Stiehm ER (1982) The DiGeorge syndrome and the fetal alcohol syndrome. Am J Dis Child 136:906–908
29. Wilson TA, Blethen SL, Vallone A, Alenick DS, Nolan P, Katz A, Amorillo TP, Goldmuntz E, Emanuel BS, Driscoll DA (1993) DiGeorge anomaly with renal agenesis in infants of mothers with diabetes. Am J Med Genet 47:1078–1082
30. Jerome LA, Papaioannou VE (2001) DiGeorge syndrome phenotype in mice mutant for the T-box gene, Tbx1. Nat Genet 27:286–291
31. Lindsay EA, Vitelli F, Su H, Morishima M, Huynh T, Pramparo T, Jurecic V, Ogunrinu G, Sutherland HF, Scambler PJ, Bradley A, Baldini A (2001) Tbx1 haploinsufficieny in the DiGeorge syndrome region causes aortic arch defects in mice. Nature 410:97–101
32. Merscher S, Funke B, Epstein JA, Heyer J, Puech A, Lu MM, Xavier RJ, Demay MB, Russell RG, Factor S, Tokooya K, Jore BS, Lopez M, Pandita RK, Lia M, Carrion D, Xu H, Schorle H, Kobler JB, Scambler P, Wynshaw-Boris A, Skoultchi AI, Morrow BE, Kucherlapati R (2001) TBX1 is responsible for cardiovascular defects in velo-cardio-facial/DiGeorge syndrome. Cell 104:619–629